HUMAN GENE THERAPY 19:887–895 (September 2008)

DOI: 10.1089/hum.2008.037

In Vivo Delivery of Bionanocapsules Displaying *Phaseolus vulgaris* Agglutinin-L_4 Isolectin to Malignant Tumors Overexpressing *N*-Acetylglucosaminyltransferase V

Takeshi Kasuya,[1] Joohee Jung,[1,2] Hiroyasu Kadoya,[1] Takashi Matsuzaki,[1,2] Kenji Tatematsu,[1] Toshihide Okajima,[1] Eiji Miyoshi,[3] Katsuyuki Tanizawa,[1,2] and Shun'ichi Kuroda[1,2]

Abstract

Metastasis is a key aspect of tumor malignancy, and several malignant tumors show expression of various mature N-type glycans. In particular, β1-6 branching *N*-acetylglucosamine (GlcNAc) is abundantly expressed as a part of high-mannose glycans in various highly metastatic cancers. *Phaseolus vulgaris* agglutinin-L_4 isolectin (L_4-PHA), which adheres to β1-6 GlcNAc specifically, has been used for *in situ* cancer diagnosis. Bionanocapsules (BNCs), hollow particles with a diameter of approximately 80 nm and composed of hepatitis B surface antigen (HBsAg) and a lipid bilayer, have been developed as human liver-specific nanocapsules for *in vivo* drug delivery system. In this study, we have generated L_4-PHA-displaying BNCs (PHA–BNCs) and examined whether L_4-PHA could retarget the BNCs to malignant tumors as a "biosensor" distinguishing tumor metastaticity. Fluorescence-labeled PHA–BNCs injected systemically into a mouse xenograft model were found to accumulate in β1-6 GlcNAc-expressing malignant tumors. The PHA–BNCs were able to deliver DNA to the malignant cancer cells. These results open up the possibility of using L_4-PHA lectin as a targeting molecule in a drug delivery system, and of using PHA–BNCs as a novel nanodevice for malignant tumor-specific bioimaging and drug delivery.

Introduction

Aberrant expression of various glycans on the surface of tumors is associated with many pathophysiological events during tumor progression, such as adhesion, proliferation, migration, apoptosis suppression, and metastasis (Hakomori, 1989). The presence on the surface of tumors of β1-6 branching *N*-acetylglucosamine (GlcNAc), which has been studied for decades, is associated with malignant transformation of rodent and human cells, and poor prognosis in cancer patients (Dennis *et al*., 1999). Either tri- or tetraantennary *N*-glycans are synthesized with *N*-acetylglucosaminyltransferase V (GnT-V) by transferring β1-6 branching GlcNAc to the trimannosyl core (Yamashita *et al*., 1985). GnT-V activity is upregulated by overexpression of proto-oncogenes (Buckhaults *et al*., 1997; Chen *et al*., 1998; Ko *et al*., 1999), and the overexpression of GnT-V in cancer cell lines has enhanced metastasis in animal models (Ihara *et al*., 2002; Murata *et al*., 2004). Metastatic tumor tissues excised from patients (e.g., colon cancer, breast cancer, melanoma, and lung cancer) have shown higher expression of GnT-V and increased amount of β1-6 GlcNAc (Fernandes *et al*., 1991; Murata *et al*., 2000; Handerson and Pawelek, 2003; Dosaka-Akita *et al*., 2004). Moreover, polyoma virus middle T antigen-induced breast tumors in *GnT-V* gene-deficient mice are much smaller than those in wild-type mice, and have shown a low incidence of metastasis (Granovsky *et al*., 2000; Dennis *et al*., 2002). These results have indicated that β1-6 GlcNAc in *N*-glycans plays crucial roles in both tumor progression and metastasis.

Some plant-derived lectins have been revealed by *in vitro* and *in vivo* studies to possess antitumor activity (Wimer, 1990; Abdullaev and De Mejia, 1997), although how lectins exhibit therapeutic effects has remained unsettled on a mo-

[1]Department of Structural Molecular Biology, Institute of Scientific and Industrial Research, Osaka University, Ibaraki, Osaka 567-0047, Japan.
[2]Japan Science and Technology Agency, Kawaguchi, Saitama 332-0012, Japan.
[3]Department of Molecular Biochemistry and Clinical Investigation, Graduate School of Medicine, Osaka University, Osaka 565-0871, Japan.

lecular basis. In particular, the kidney bean-derived lectin, *Phaseolus vulgaris* agglutinin-L_4 (L_4-PHA), has been administered intravenously to cancer patients, and has shown a weak therapeutic effect without severe side effects (Wimer, 1997). L_4-PHA has been used for cancer diagnosis, specifically *in situ* histological analysis to identify β1-6 GlcNAc-expressing malignant cancer cells (Cumming and Kornfeld, 1982; Raedler and Shreiber, 1988). These applications strongly suggest that L_4-PHA possesses both sufficient safety in cancer patients and high affinity for malignant tumors, and led us to examine whether L_4-PHA is capable of delivering drug delivery system (DDS) carriers to malignant tumors *in vivo* by systemic administration.

A bionanocapsule (BNC) is a hollow particle about 80 nm in diameter and composed of about 130 molecules of hepatitis B virus (HBV) surface antigen (HBsAg) L proteins and a lipid bilayer (Kuroda *et al*., 1992; Yamada *et al*., 2001). The N-terminal outer membrane region (pre-S region) of HBsAg is indispensable for the attachment of HBV to human liver cells (Neurath *et al*., 1986), and the C-terminal transmembrane region (S), including a membrane-fusion peptide sequence (Berting *et al*., 2000), interacts with cellular endocytosis-related proteins (Mehdi *et al*., 1994; De Meyer *et al*., 1999). These regions are postulated to contribute concurrently to human liver-specific infection with HBV. Various materials (e.g., DNA, chemicals, and polystyrene beads) can be incorporated by either electroporation (Yamada *et al*., 2003; Iwasaki *et al*., 2007) or liposome conjugation (Jung *et al*., 2008). Intravenous injection of BNCs has allowed the efficient delivery of incorporated payloads to human liver-derived cells and tumors by using the HBV infection machinery (Yamada *et al*., 2003; Iwasaki *et al*., 2007; Jung *et al*., 2008). The cell and tissue specificity of BNCs can be altered by replacing the pre-S region with other targeting molecules: for example, epidemical growth factor (EGF) for EGFR (EGF receptor)-expressing cells (Yamada *et al*., 2003), and anti-EGFR antibody for EGFR-expressing tumors (Tsutsui *et al*., 2007). Thus, BNCs have facilitated the *in vivo* pinpoint delivery of various materials to cells and tissues of interest.

In this study, we have generated L_4-PHA-displaying BNCs (PHA–BNCs) by means of the avidin–biotin conjugation system to target malignant cancer cells (GnT-V-overexpressing cells) in cultured cells (*ex vivo*) and a mouse xenograft model (*in vivo*).

Materials and Methods

Preparation of L_4-PHA-displaying BNCs

The BNC-harboring HBsAg mutant, the pre-S region of which was replaced with an IgG Fc-binding motif derived from *Staphylococcus aureus* protein A (Tsutsui *et al*., 2007), was produced as described previously (Yamada *et al*., 2003). Purified BNCs were biotinylated with sulfonated *N*-hydroxysulfosuccinimide (NHS)–biotin (Pierce Biotechnology, Rockford, IL). Biotinylated BNCs (bio-BNCs) were purified with a Zeba desalt spin column (Pierce Biotechnology). Biotinylated lectin (*Phaseolus vulgaris* agglutinin-L_4; L_4-PHA) obtained from Seikagaku (Tokyo, Japan), was mixed with an equimolar amount of streptavidin (SA; Seikagaku) and incubated for 10 min at room temperature to produce SA-conjugated PHA (SA–PHA) complex. The complex was mixed with an equimolar amount of bio-BNCs (as HBsAg protein) for 30 min at room temperature to produce L_4-PHA lectin-displaying BNCs (PHA–BNCs).

Quartz crystal microbalance analysis and size measurement of PHA–BNCs

The weight of protein displayed on the BNC surface was quantitated by quartz crystal microbalance (QCM) at 25°C, using a Twin-Q (As One Corp., Osaka, Japan), which has two 500-μl cells equipped with 27-MHz QCM plates. Bio-BNCs (about 100 ng as HBsAg protein) were immobilized on a gold electrode, and the electrode was washed and blocked with skim milk at a final concentration of 0.04% (w/v). The adsorption of SA onto bio-BNCs and the additional absorption of bio-PHA onto SA–BNCs were monitored by frequency change, with 1 Hz corresponding to 30 pg of absorbed protein. The size distribution and average size of PHA–BNCs were determined in phosphate-buffered saline (PBS) at 25°C by dynamic light scattering, using a Zetasizer model Nano-ZS (Malvern Instruments, Worcestershire, UK). The polydispersity index (PDI) is a width parameter for *z*-average as an intensity mean.

Immunoprecipitation

PHA–BNCs (20 μg as HBsAg protein) was incubated for 5 min at room temperature with 1 ml of PBS containing 5% (w/v) bovine serum albumin (BSA) and 0.01% (v/v) Triton X-100, mixed with mouse monoclonal anti-S region IgG-conjugated microbeads (20 μl, 50% [v/v] slurry) supplied as the IMx HBsAg assay system (Abbott Japan, Tokyo, Japan), and incubated for 5 min at room temperature. The microbeads were washed three times with PBS containing 5% BSA and 0.01% Triton X-100, boiled in Laemmli sample buffer for 15 min, and analyzed by Western blotting with horseradish peroxidase-conjugated SA (HRP–SA; GE Healthcare, Giles, Buckinghamshire, UK) and the enhanced chemiluminescence method (ECL Plus; GE Healthcare).

Cells

The human colon adenocarcinoma cell line WiDr and the human gastric cancer cell line MKN45 were cultured in Dulbecco's minimal essential medium (DMEM) supplemented with 10% (v/v) fetal bovine serum (FBS). GnT-V-expressing stable cell lines, WiDr-GnT-V (Murata *et al*., 2004) and MKN45-GnT-V (Ihara *et al*., 2002), were cultured in the same medium containing G418 (300 μg/ml; Nakalai Tesque, Kyoto, Japan).

Lectin blotting

Cells were lysed with 50 m*M* Tris-HCl (pH 8.0) containing 1 m*M* EDTA, 1 m*M* dithiothreitol, and 1% (v/v) Triton X-100. A blot containing 10 μg of lysate (as protein) in each lane was blocked overnight at 4°C with PBS containing 3% (w/v) BSA, incubated with bio-PHA (1 μg/ml) for 1 hr at room temperature, washed three times with PBS containing 0.01% Triton X-100, and then visualized with HRP–SA and ECL Plus.

Cytochemical analysis with L_4-PHA lectin

Cells (about 1×10^5) were cultured on a 24-well plate (BD Biosciences, San Jose, CA) for 24 hr, washed twice with ice-

cold PBS, and kept on ice in complete medium containing bio-PHA (1 μg/ml) for 1 hr. Cells were washed twice with ice-cold PBS, fixed with 4% (w/v) paraformaldehyde in PBS for 15 min at room temperature, stained with Alexa 488-labeled SA (0.2 μg/ml; Invitrogen, Carlsbad, CA) and Hoechst 33342 (2.5 μg/ml) for 1 hr at room temperature, washed three times with PBS, and then observed under a confocal laser microscope (FV-1000D; Olympus, Tokyo, Japan).

Ex vivo *delivery of PHA–BNCs*

Bio-BNCs were labeled with a membrane probe, 1,1′-dioctadecyl-3,3,3′,3′-tetramethylindodicarbocyanine, 4-chlorobenzenesulfonate (DiD; Invitrogen) (excitation at 644 nm, emission at 665 nm), passed through a Zeba desalt spin column, and then conjugated with SA–PHA. Cells (about 1×10^5) were cultured on a 24-well plate for 24 hr and incubated with DiD-labeled PHA–BNCs (5 μg as HBsAg protein) for 3 hr in complete medium. Delivery of PHA–BNCs was observed as described above. For flow cytometric analysis, the cells incubated with DiD-labeled PHA–BNCs were washed with PBS, treated with 0.25% (w/v) trypsin–EDTA for 15 min at 37°C, and washed with ice-cold PBS three times. The cells were analyzed with a FACSCanto II (BD Biosciences) equipped with 633-nm excitation laser and 660-nm long-path filter. Thirty thousand cells were counted in each sample. The obtained data were analyzed with FlowJo software (Tree Star, Ashland, OR).

In vivo *optical imaging*

All animal experiments were approved by the committee for experimental animal science of the Institute of Scientific and Industrial Research (Osaka University, Osaka, Japan). Animals were treated according to the guidelines of the Ministry of Education, Culture, Sports, Science, and Technology, Japan. Either WiDr-GnT-V cells or WiDr cells (about 1×10^5) were suspended in 100 μl of DMEM containing 10% (v/v) BD Matrigel matrix HC (BD Biosciences) and injected subcutaneously into the backs of BALB/c (*nu/nu*) nude mice (5 weeks old, male; CLEA, Tokyo, Japan). When tumors reached about 1 cm in diameter, DiD-labeled PHA–BNCs (40 μg as HBsAg protein) were injected through the tail vain. One, 4, 8, 16, 24, and 48 hr after injection, whole-body fluorescence was observed with an *in vivo* optical imaging system (OV100; Olympus). Twenty-four hours after injection, the mice were killed; livers, hearts, and tumors were isolated surgically, and their fluorescence was observed similarly. Fluorescence intensity was analyzed with Wasabi software (Hamamatsu Photonics, Hamamatsu, Japan). The number of mice in each group was three.

Ex vivo *gene delivery*

Incorporation of DNA into BNCs was performed by the BNC–liposome complex method (Jung *et al.*, 2008). Briefly, a freeze-dried form of cationic liposomes (1.5 mg as lipids; Coatsome EL-01-D; NOF, Tokyo, Japan) was mixed with firefly-derived luciferase expression vector pGL3 (250 μg; Promega, Madison, WI) to form the lipoplex (liposome–DNA complex). Aliquots (100 μg of liposomes, 16.7 μg of DNA) were incubated with bio-BNCs (100 μg as HBsAg protein) for 30 min at room temperature to allow the formation of a BNC–liposome–DNA complex. About 1×10^5 cells in a 24-well plate were incubated with the complex (1 μg as HBsAg protein) for 3 hr and cultured in fresh complete medium for 72 hr; and then the luciferase activity of each cell lysate was measured with a luciferase assay system (Promega).

Results

Preparation of BNCs displaying L_4-PHA lectin

Purified BNCs were biotinylated with sulfonated NHS–biotin, and conjugated with SA-conjugated L_4-PHA (SA–PHA) to produce L_4-PHA-displaying BNCs (PHA–BNCs). The amount of protein displayed on the bio-BNC surface was measured with a quartz crystal microbalance (QCM). On the basis of the change in oscillation frequency of the quartz crystal, the amount of SA displayed on 1 mol of BNCs was calculated as 35.6 mol. Because the number of HBsAg molecules embedded in the BNC lipid bilayer is about 130 (M. Iijima and S. Kuroda, unpublished observations; *see* Yamada *et al.*, 2001), 1 mol of HBsAg was estimated to bind with 0.32 mol of SA. Similarly, 5.7 mol of bio-PHA was estimated to bind with 1 mol of SA–BNCs. Next, the average sizes of bio-BNCs, SA–BNCs, and PHA–BNCs were determined by dy-

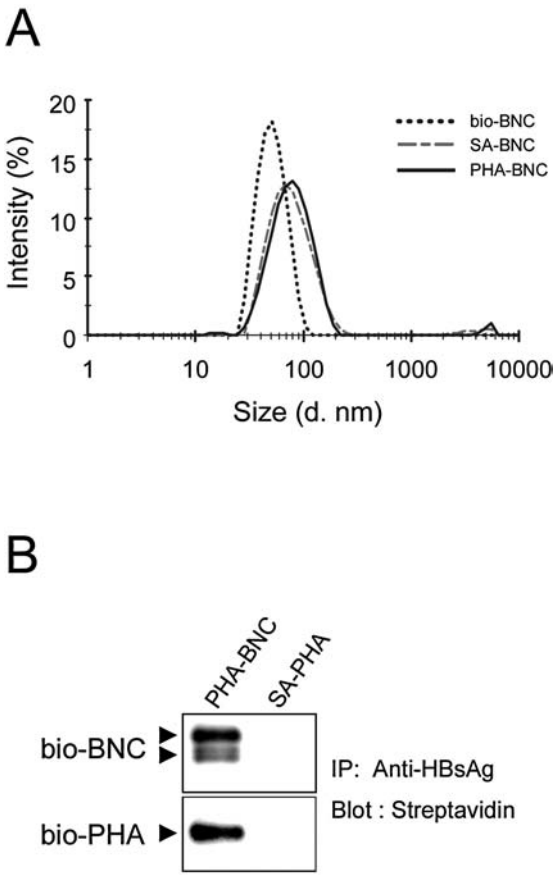

FIG. 1. Preparation of PHA–BNCs. (**A**) The diameters (nm) of bio-BNCs (dotted line), SA–BNCs (dashed line), and PHA–BNCs (solid line) were measured by dynamic light scattering (3 batches, 12 measurements for each batch). (**B**) PHA–BNCs and SA–PHA (negative control) were immunoprecipitated with an anti-HBsAg antibody, and analyzed by Western blotting with HRP–SA.

namic light scattering as 48.5 nm (PDI, 0.086), 70.6 nm (PDI, 0.179), and 74.9 nm (PDI, 0.225), respectively (Fig. 1A). To confirm the display of L_4-PHA molecule on BNCs, PHA–BNCs were immunoprecipitated with anti-HBsAg (S region) IgG-conjugated microbeads and subjected to Western blotting with HRP–SA. As shown in Fig. 1B, both bio-BNCs (about 45 and 48 kDa; the size difference is caused by glycosylation) and bio-PHA (about 30 kDa) were found to be coimmunoprecipitated, indicating that both molecules successfully form a complex on the surface of BNCs.

Identification of β1-6 GlcNAc in GnT-V-overexpressing cells

GnT-V-overexpressing stable cell lines WiDr and MKN45 (WiDr-GnT-V and MKN45-GnT-V) were analyzed by lectin blot and cytochemistry using L_4-PHA lectin. Increased amounts of β1-6 GlcNAc were found in 80- to 100-kDa and about 150- to 200-kDa proteins in the WiDr-GnT-V and MKN45-GnT-V cell lines, respectively (Fig. 2A, left). The protein profile of neither cell line was significantly changed by overexpression of GnT-V (Fig. 2A, right). GnT-V expression induced the change from β1-6 GlcNAc-free *N*-glycans to β1-6 GlcNAc-containing *N*-glycans, and it was considered that both amount and size of *N*-glycoproteins were not significantly affected by GnT-V expression. Cytochemical analyses using L_4-PHA lectin also confirmed that the expression of β1-6 GlcNAc on the cell surface is significantly enhanced in GnT-V-overexpressing cell lines (Fig. 2B). On the basis of the fluorescence intensity, the WiDr-GnT-V cell line was considered to express a greater amount of β1-6 GlcNAc on its surface compared with the MKN45-GnT-V cell line.

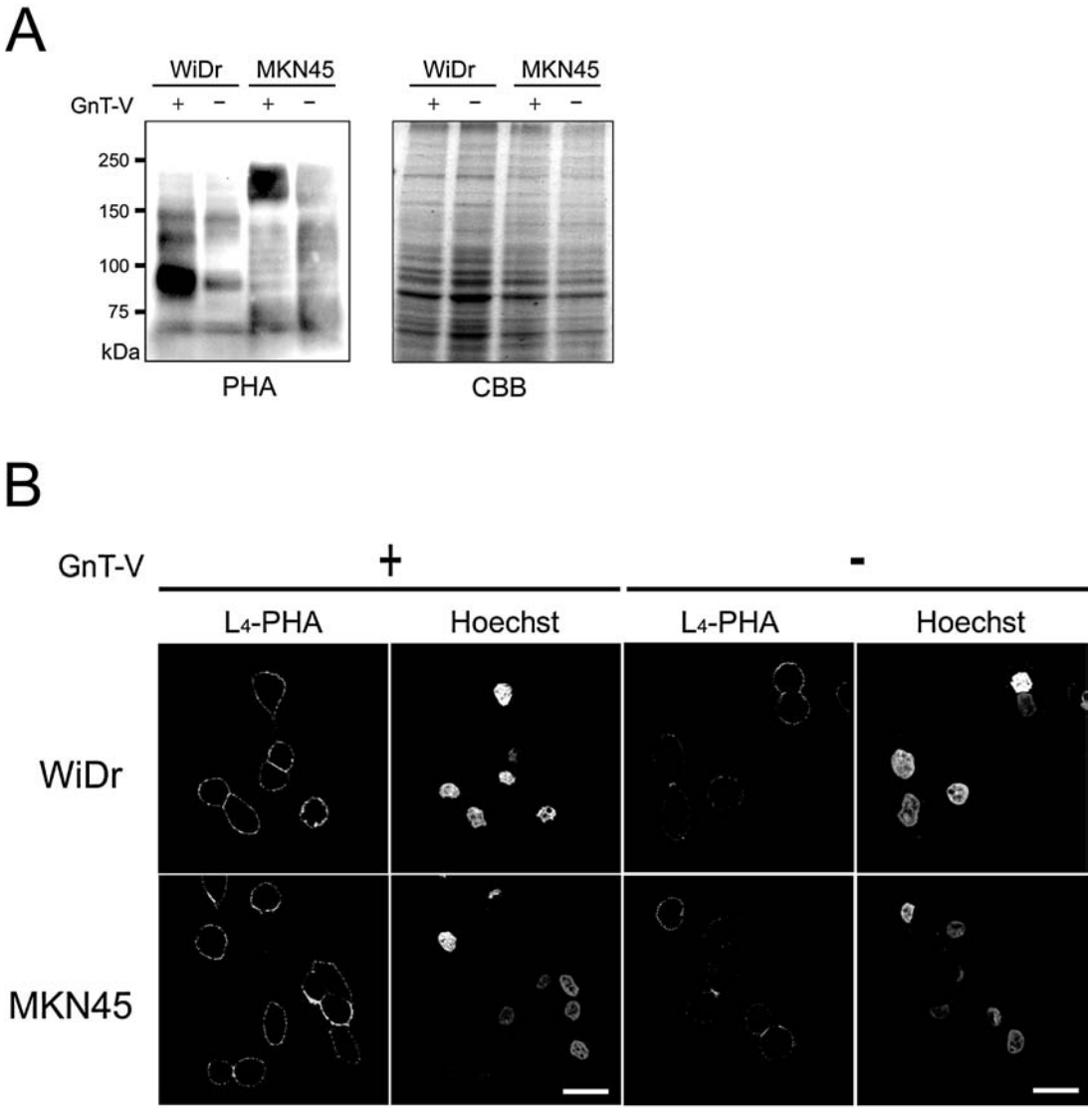

FIG. 2. Expression of β1-6 GlcNAc in GnT-V-overexpressing cells. (**A**) Ten micrograms (as protein) of total cell lysate (WiDr, MKN45 with/without GnT-V expression) was subjected to sodium dodecyl sulfate–polyacrylamide gel electrophoresis, and analyzed by lectin blotting with L_4-PHA (*left*) and Coomassie Brilliant Blue R-250 (CBB) staining (*right*). (**B**) Cytochemical analyses of GnT-V-overexpressing cells, using L_4-PHA lectin and Hoechst 33342. Scale bars: 20 μm.

L_4-PHA-mediated ex vivo *accumulation of BNCs*

To examine whether L_4-PHA could deliver BNCs to target cells *ex vivo*, the lipid bilayer moiety of PHA–BNCs was labeled with DiD, a membrane probe, and DiD-labeled PHA–BNCs were directly added to the culture medium of GnT-V-overexpressing cell lines. After 3 hr, strong DiD-derived fluorescence was found in both GnT-V-overexpressing cell lines (Fig. 3A). Cytotoxicity was not observed by phase-contrast imaging. This result suggested that a remarkable amount of PHA–BNCs accumulated in GnT-V-overexpressing cells, presumably through the interaction of L_4-PHA with cell surface β1-6 GlcNAc. The weak fluorescence observed in both parental cell lines might have been caused by endogenous β1-6 GlcNAc, as observed in Fig. 2A. Intriguingly, the fluorescence of the WiDr-GnT-V cell line was higher than that of the MKN45-GnT-V cell line, which may be due to the lower amount of β1-6 GlcNAc in the MKN45-GnT-V cell line (*see* Fig. 2B). Flow cytometric analysis (Fig. 3B) confirmed that the GnT-V-overexpressing cell lines showed stronger

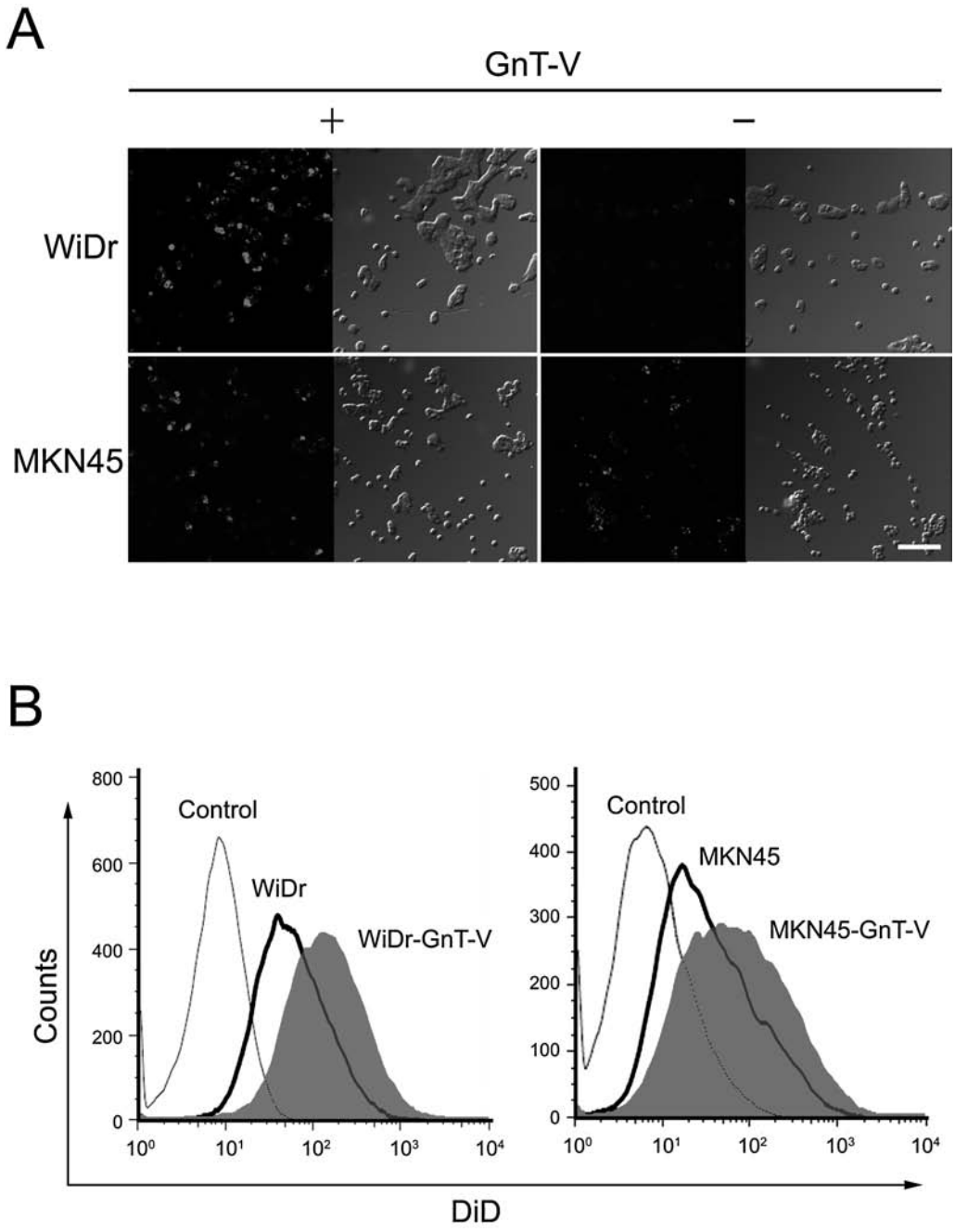

FIG. 3. L_4-PHA-mediated *ex vivo* accumulation of BNC. (**A**) Either GnT-V-overexpressing or parental cells of WiDr and MKN45 were incubated with DiD-labeled PHA–BNC, and then observed 3 hr after administration. Scale bar: 100 μm. (**B**) The cells incubated with DiD-labeled PHA–BNC were analyzed by flow cytometry. Untreated GnT-V-overexpresssing cells were used as control.

fluorescence intensity than parental WiDr and MKN45 cells. Geometric mean fluorescence intensity in GnT-V-overexpressing cells was approximately 2.6- and 1.9-fold higher than that of parental WiDr and MKN45 cells, respectively. Collectively, PHA–BNCs were shown to accumulate specifically with β1-6 GlcNAc-overexpressing cells *ex vivo* because of the targeting ability of L_4-PHA.

L_4-PHA-mediated in vivo *delivery of BNCs*

The mouse xenograft model harboring WiDr- and WiDr-GnT-V-derived tumors was used to evaluate the targeting ability of PHA–BNCs *in vivo*. Mice received systemic administration of DiD-labeled PHA–BNCs (40 μg as BNC protein) via the tail vein, and then the DiD-derived fluorescence from tumors was investigated with the *in vivo* optical imaging system 0, 1, 4, 8, 16, 24, and 48 hr after injection (Fig. 4A). Fluorescence was initially detected in WiDr-GnT-V-derived tumors at 1 hr, and reached a maximum at 24 hr (Fig. 4A, left). A slight increase in fluorescence was observed in WiDr-derived tumors during the observation period (Fig. 4A, right), implying that the enhanced permeability retention (EPR) effect is nearly undetectable in this system. To confirm the β1-6 GlcNAc-dependent accumulation of PHA–BNCs, mice were killed 24 hr after injection and tumors, hearts, and livers were isolated and observed with the *in vivo* optical imaging system. DiD-derived fluorescence was observed in both tumor types; GnT-V-overexpressing tumors showed higher fluorescence intensity than control tumors (Fig. 4B, top). However, the fluorescence intensities of both GnT-V-overexpressing and control liver showed no significant difference (Fig. 4B, bottom), indicating that PHA–BNCs might be equally trapped by the reticuloendothelial system (RES) in both livers. Among other major organs (spleen, kidney, heart, and lung), heart (Fig. 4B, middle) and kidneys showed weaker fluorescence than liver, but stronger than spleen and lungs. Regardless of the expression of GnT-V in tumors, there was no difference in the fluorescence of these organs. These results indicate that PHA–BNCs can efficiently accumulate in β1-6 GlcNAc-overexpressing tumor *in vivo* even by systemic administration.

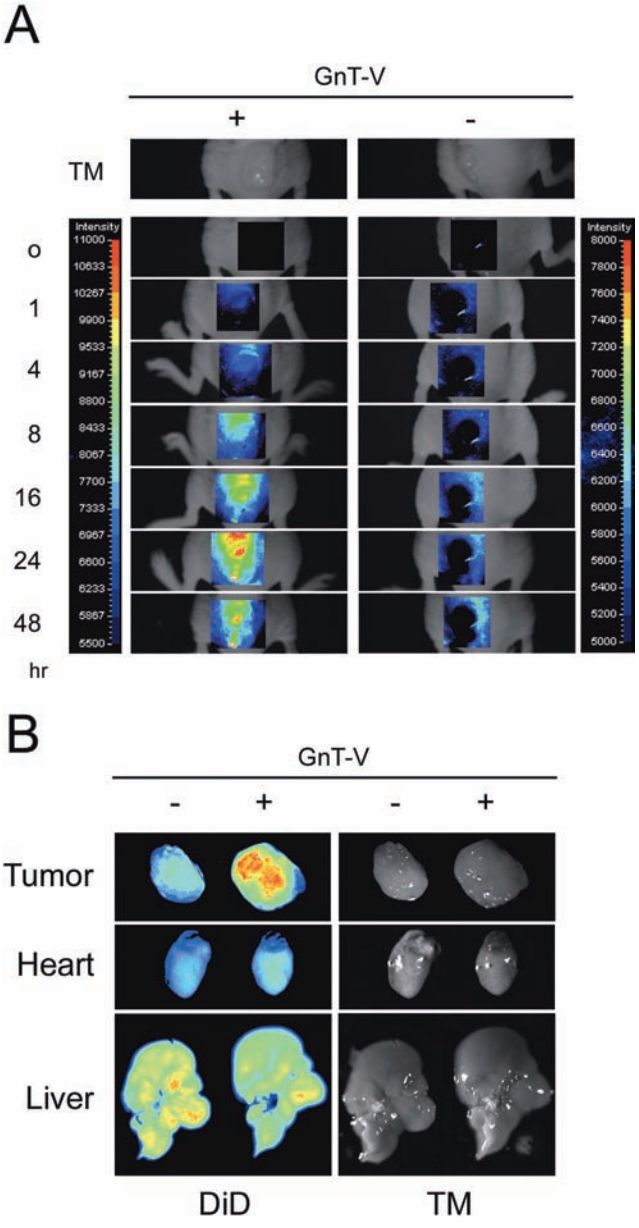

FIG. 4. L_4-PHA-mediated *in vivo* delivery of BNC. (**A**) The tumor region was observed with an *in vivo* imaging system after systemic administration of DiD-labeled PHA–BNC. The number of mice in each group was three. Similar results were obtained from each mouse. TM, transmission image. (**B**) Tumors, hearts, and livers were isolated and observed with an *in vivo* imaging system 24 hr after administration.

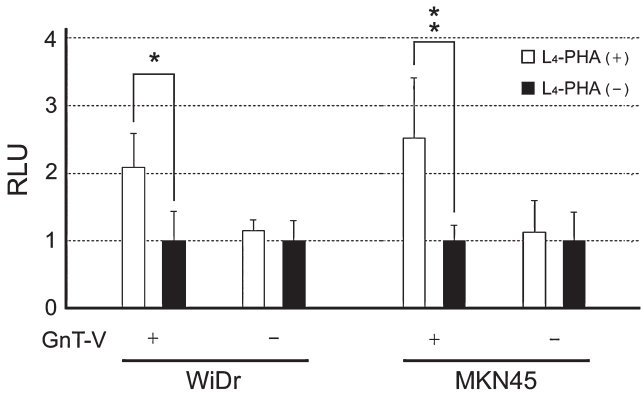

FIG. 5. L_4-PHA-mediated *ex vivo* gene delivery. Cells incubated with BNC–liposome complexes were lysed, and luciferase activity was measured. Results are presented as relative luminescence units (RLU) normalized to the protein concentration. The relative luminescence units derived for each cell line treated with bio-BNC–liposome complexes [L_4-PHA(–)] was set as 1 ($n = 4$; mean ± SD; t test, $^*p < 0.05$, $^{**}p < 0.005$).

L_4-PHA-mediated ex vivo *gene delivery*

Our studies have shown that BNCs form complexes with liposomes (Jung *et al*., 2008), so that liposomes containing various materials (e.g., DNA, chemicals, or polystyrene beads) could be conjugated with BNCs, and then the BNC–liposome complexes could transport the incorporated payloads to target cells *ex vivo* and *in vivo*, based on the speci-

ficity of the BNCs. We therefore examined the transfection efficiency of a PHA–BNC–liposome complex to the malignant cancer cell lines WiDr-GnT-V and MKN45-GnT-V, using a luciferase gene as a reporter (Fig. 5). Both PHA–BNCs and bio-BNCs (negative control) showed similar luciferase activities in parental cell lines. PHA–BNCs were revealed to possess higher transfection efficiency to the GnT-V-overexpressing cell lines. Thus, PHA–BNC–liposome complexes can transport incorporated genes specifically to β1-6 GlcNAc-overexpressing malignant cell lines.

Discussion

Several lectins have so far been recognized as useful molecules for the diagnosis of various tumors *in situ* and *in vivo* (e.g., HPA [*Helix pomatia* agglutinin] for imaging tumors [Debbage *et al*., 1998] and L_4-PHA in tumor diagnosis [Raedler and Schreiber, 1988] and in the treatment of cancers in human ([Wimer, 1997]). As for the delivery of anticancer drugs, a few attempts have been made with lectins. Wheat germ agglutinin (WGA)-conjugated liposomes have been used to deliver cisplatin to radiation-induced endothelial inflammatory areas in tumors by systemic administration (Geng *et al*., 2004). However, the WGA-conjugated liposomes could not be used without the pretreatment with radiation. In this study, it was demonstrated that L_4-PHA is applicable for the targeting of BNCs to β1-6 GlcNAc-overexpressing malignant tumors *ex vivo* and *in vivo* without any additional pretreatment. Because expression of the β1-6 GlcNAc moiety is widely spread among highly metastatic tumors in humans (Fernandes *et al*., 1991; Handerson and Pawelek, 2003; Dosaka-Akita *et al*., 2004), PHA–BNCs are considered a promising nanodevice for either *in vivo* pinpoint gene/drug delivery in cancer therapy or bioimaging in cancer diagnosis.

The size of nanodevices in this field of research is generally important for *in vivo* systemic administration, because too large a device (>150 nm in diameter) will be removed from the bloodstream by the macrophages of the liver and spleen (i.e., RES) and too small a device (<40 nm in diameter) is also filtrated by the kidney (Drummond *et al*., 1999). Moreover, the pore size of the tumor vasculature varies from 100 to 780 nm, which is larger than that of normal tissues (Hobbs *et al*., 1998). Therefore, the diameter of nanodevices must be less than 200 nm for efficient capture by the tumor vasculature (i.e., EPR effect) (Sinn *et al*., 2005). The average diameter of PHA–BNCs, about 75 nm (*see* Fig. 1A), is considered appropriate for *in vivo* tumor targeting. As shown in Fig. 4B, a substantial amount of PHA–BNCs was found to accumulate in the liver, indicating that RES unexpectedly entrapped PHA–BNCs. To avoid this entrapment and to improve the blood retention time, various nanodevices have been modified with polyethylene glycol (PEG) (Portney and Ozkan, 2006). The biodistribution of PHA–BNCs may be optimized by a PEG modification to achieve an effective cancer treatment.

BNC–liposome complexes could deliver incorporated payloads to specific cells and tissues *in vivo* by the targeting ability of BNCs (Jung *et al*., 2008). In this study we generated bio-BNCs displaying L_4-PHA on their surface, which has allowed us to display various targeting molecules (e.g., cytokines, glycans, peptides, and antibodies) and to expand the applications of BNCs and BNC–liposome complexes. The transfection process based on BNCs and BNC–liposome complexes is postulated to consist of two steps. First, the target cell is recognized by the targeting molecules displayed on BNCs, such as the pre-S region for human hepatocytes (Yamada *et al*., 2003; Iwasaki *et al*., 2007; Jung *et al*., 2008), EGF for EGFR-expressing cells (Yamada *et al*., 2003), or anti-EGFR antibody for EGFR-expressing cells (Tsutsui *et al*., 2007). Second, the disintegration of BNCs occurs on the cellular membrane followed by the action of membrane-fusion peptide sequences in pre-S and S regions (Berting *et al*., 2000; Oess and Hildt, 2000), and the payloads are released into the cytoplasm (Jung *et al*., 2008). Because PHA–BNC–liposome complexes successfully delivered DNA to GnT-V-overexpressing cells (*see* Fig. 5), presumably the complexes were captured by the β1-6 GlcNAc moiety on the target cells and then the payload was released to the cytoplasm.

As for tumor-directed *in vivo* delivery of nanodevices containing therapeutic materials to cancers, various targeting molecules have so far been displayed on the surface of such nanodevices, including antibodies (Schliemann and Neri, 2007), homing peptides (Zurita *et al*., 2003), and aptamers (Ireson and Kelland, 2006). These molecules contribute to deliver the adjunct nanodevices by recognizing cell surface proteins; however, the recognition of targeting molecules is sometimes dependent on the species. This situation has hampered the development of these nanodevices for clinical use, although these nanodevices show high efficacy in animal models (Marshall, 2006). On the other hand, the structure of *N*-glycans is highly conserved between rodents and humans; in particular, the aberrant expression of β1-6 GlcNAc in malignant cancers has been observed in both murine models and humans. Our new strategy using lectins to target abnormal glycans, as hallmarks of malignant cancer, may indicate a novel DDS for cancer therapy.

Acknowledgments

The authors thank Dr. T. Yamada (Beacle, Inc.), Prof. M. Seno (Okayama University), Prof. A. Kondo (Kobe University), and Prof. M. Ueda (Keio University, Medical School) for helpful advice. The authors are also grateful to Ms. Y. Matsushita for technical support. This work was supported in part by Grants-in-Aid for Scientific Research on Priority Areas (18015032) from the Ministry of Education, Culture, Sports, Science, and Technology of Japan; Creation of Bio-Devices and Bio-Systems with Chemical and Biological Molecules for Medical Use (CREST) and the Regional Research and Development Resources Utilization Program of the Japan Science and Technology Agency (JST); and by Grants-in-Aid for Research on Advanced Medical Technology from the Ministry of Health, Labor, and Welfare.

Author Disclosure Statement

No competing financial interests exist.

References

Abdullaev, F.I., and De Mejia, E.G. (1997). Antitumor effect of plant lectins. Natural Toxins 5, 157–163.

Berting, A., Fischer, C., Schaefer, S., Garten, W., Klenk, H.D., and Gerlich, W.H. (2000). Hemifusion activity of a chimeric in-

fluenza virus hemagglutinin with a putative fusion peptide from hepatitis B virus. Virus Res. 68, 35–49.

Buckhaults. P., Chen, L., Freigen, N., and Pierce, M. (1997) Transcriptional regulation of *N*-acetylglucosaminyltransferase V by the *src* oncogene. J. Biol. Chem. 272, 19575–19581.

Chen, L., Zhang, W., Fregien, N., and Pierce, M. (1998). The Her-2/*neu* oncogene stimulates the transcription of *N*-acetylglucosaminyltransferase V and expression of its cell surface oligosaccharide products. Oncogene 17, 2087–2093.

Cummings, R.D., and Kornfeld, S. (1982). Characterization of the structural determinants required for the high affinity interaction of asparagine-linked oligosaccharides with immobilized *Phaseolus vulgaris* leukoagglutinating and erythroagglutinating lectins. J. Biol. Chem. 257, 11230–11234.

Debbage, P.L., Griebel, J., Ried, M., Gneiting, T., De Vries, A., and Hulzler, P. (1998). Lectin intravital perfusion studies in tumor-bearing mice: Micrometer-resolution, wide-area mapping of microvascular labeling, distinguishing efficiently and inefficiently perfused microregions in the tumor. J. Histochem. Cytochem. 46, 627–639.

De Meyer, S., Depla, E., Maertens, G., Soumillion, S., and Yap, S.H. (1999). Characterization of small hepatitis B surface antigen epitopes involved in binding to human annexin V. J. Viral Hepat. 6, 277–285.

Dennis, J.S., Pawling, J., Cheung, P., Partridge, E., and Demetriou, M. (2002). UDP-*N*-acetylglucosamine:α-6-D-mannoside β1,6 *N*-acetylglucosaminyltransferase V (Mgat5) deficient mice. Biochim. Biophys. Acta 1573, 414–422.

Dennis, J.W., Granovsky, M., and Warren, C.E. (1999). Glycoprotein glycosylation and cancer progression. Biochim. Biophys. Acta 1473, 21–34.

Dosaka-Akita, H., Miyoshi, E., Suzuki O., Itoh, T., Katoh, H., and Taniguchi, N. (2004). Expression of *N*-acetylglucosaminyltransferase V is associated with prognosis and histology in non-small cell lung cancers. Clin. Cancer Res. 10, 1773–1779.

Drummond, D.C., Meyer, O., Hong, K., Kirpotin, D., and Papahadjopoulos, D. (1999). Optimizing liposomes for delivery of chemotherapeutic agents to solid tumors. Pharm. Rev. 51, 691–743.

Fernandes, B., Sagman, U., Auger, M., Demetriou, M., and Dennis, J.W. (1991). β1-6 branched oligosaccharides as a marker of tumor progression in human breast and colon neoplasia. Cancer Res. 51, 718–723.

Geng, L., Osusuky, K., Konjeti, S., Fu, A., and Hallahan, D. (2004). Radiation-guided drug delivery to tumor blood vessels results in improved tumor growth delay. J. Control. Release 99, 369–381.

Granovsky, M., Faya, J., Pawling, J., Mullar, J., Khokha, R., and Dennis, J.W. (2000). Suppression of tumor growth and metastasis in Mgat5-deficient mice. Nat. Med. 6, 306–312.

Hakomori, S. (1989). Aberrant glycosylation in tumors and tumor-associated carbohydrate antigens. Adv. Cancer Res. 52, 257–331.

Handerson, T., and Pawelek, J.M. (2003). β1,6-branched oligosaccharides and coarse vesicles: A common, pervasive phenotype in melanoma and other human cancers. Cancer Res. 63, 5363–5369.

Hobbs, S.K., Monsky, W.L., Yuan, F., Roberts, W.G., Griffith, L., Torchilin, V.P., and Jain, R.K. (1998). Regulation of transport pathways in tumor vessels: Role of tumor type and microenvironment. Proc. Natl. Acad. Sci. U.S.A. 95, 4607–4612.

Ihara, S., Miyoshi, E., Ko, J.H., Murata, K., Nakahara, S., Honke, K., Dickson, R.B., Lin, C.Y., and Taniguchi, N. (2002). Prometastatic effect of *N*-acetylglucosaminyltransferase V is due to modification and stabilization of active matriptase by adding β1-6 GlcNAc branching. J. Biol. Chem. 277, 16960–16967.

Ireson, C.R., and Kelland, L.R. (2006). Discovery and development of anticancer aptamers. Mol. Cancer Ther. 12, 2957–2962.

Iwasaki, Y., Ueda, M., Yamada, T., Kondo, A., Seno, M., Tanizawa, K., Kuroda, S., Sakamoto, M., and Kitajima, M. (2007). Gene therapy of liver tumors with human liver-specific nanoparticles. Cancer Gene Ther. 14, 74–81.

Jung, J., Matsuzaki, T., Tatematsu, K., Okajima, T., Tanizawa, K., and Kuroda, S. (2008). Bio-nanocapsule conjugated with liposomes for *in vivo* pinpoint delivery of various materials. J. Control. Release 126, 255–264.

Ko, J.H., Miyoshi, E., Noda, K., Ekuni, A., Kang, R., Ikeda, Y., and Taniguchi, N. (1999). Regulation of the GnT-V promoter by transcription factor Ets-1 in various cancer cell lines. J. Biol. Chem. 274, 22941–22948.

Kuroda, S., Otaka, S., Miyazaki, T., Nakao, M., and Fujisawa, Y. (1992). Hepatitis B virus envelope L protein particles: Synthesis and assembly in *Saccharomyces cerevisiae*, purification and characterization. J. Biol. Chem. 267, 1953–1961.

Marshall, E. (2006) Violent reaction to monoclonal antibody therapy remains a mystery. Science 311, 1688–1689.

Mehdi, H., Kaplan, M.J., Anlar, F.Y., Yang, X., Bayer, R., Sutherland, K., and Peeples, M.E. (1994). Hepatitis B virus surface antigen binds to apolipoprotein H. J. Virol. 68, 2415–2424.

Murata, K., Miyoshi, E., Kameyama, M., O. Ishikawa, Kabuto, T., Sasaki, Y., Hiratsuka, M., Ohigashi, H., Ishiguro, S., Ito, S., Honda, H., Takemura, F., Taniguchi, N., and Imaoka, S. (2000). Expression of *N*-acetylglucosaminyltransferase V in colorectal cancer correlates with metastasis and poor prognosis. Clin. Cancer Res. 6, 1772–1777.

Murata, K., Miyoshi. E., Ihara, Noura, S., Kameyama, M., Ishikawa, O., Doki, Y., Yamada, T., Ohigashi, H., Sasaki, Y., Higashiyama, M., Tarui, T., Takeda, Y., Kannagi, R., Taniguchi, N., and Imaoka, S. (2004). Attachment of human colon cancer cells to vascular endothelium is enhanced by *N*-acetylglucosaminyltransferase V. Oncology 66, 492–501.

Neurath, A.R., Kent, S.B., Strick, N., and Parker, K. (1986). Identification and chemical synthesis of a host cell receptor binding site on hepatitis B virus. Cell 46, 429–436.

Oess, S., and Hildt, E. (2000). Novel cell permeable motif derived from the PreS2-domain of hepatitis-B virus surface antigens. Gene Ther. 7, 750–758.

Portney, N.G., and Ozkan, M. (2006). Nano-drug delivery, imaging, and sensing. Anal. Bioanal. Chem. 384, 620–630.

Raedler, A., and Schreiber, S. (1988). Analysis of differentiation and transformation of cells by lectins. Crit. Rev. Clin. Lab. Sci. 26, 153–193.

Schliemann, C., and Neri, D. (2007). Antibody-based targeting of the tumor vasculature. Biochim. Biophys. Acta 1776, 175–192.

Sinn, P.L., Sauter, S.L., and McCray, P.B., Jr. (2005). Gene therapy progress and prospects: Development of improved lentiviral and retroviral vectors: design, biosafety, and production. Gene Ther. 12, 1089–1098.

Tsutsui, Y., Tomizawa, K., Nagita, M., Michiue, H., Nishiki, T., Ohmori, I., Seno, M., and Matsui, M. (2007). Development of bionanocapsules targeting brain tumors. J. Control. Release 122, 159–164.

Wimer, B.M. (1990). Therapeutic activities of PHA-L_4, the mitogenic isolectin of phytohemagglutinin. Mol. Biother. 2, 74–90.

Wimer, B.M. (1997). Therapeutic immunostimulating effects of plant mitogens exemplified by the L_4 isolectin of PHA. Cancer Biother. Radiopharm. 12, 195–212.

Yamada, T., Iwabuki, H., Kanno T., Tanaka, H., Kawai, T., Fukuda, H., Kondo, A., Seno, M., Tanizawa, K., and Kuroda, S. (2001). Physicochemical and immunological characterization of hepatitis B virus envelope particles exclusively consisting of the entire L (pre-S1 + pre-S2 + S) protein. Vaccine 19, 3154–3163.

Yamada, T., Iwasaki, Y., Tada, H., Iwabuki, H., Chuah, M.K., Vandendriessche, T., Fukuda, H., Kondo, A., Ueda, M., Seno, M., Tanizawa, K., and Kuroda, S. (2003). Nanoparticles for the delivery of genes and drugs to human hepatocytes. Nat. Biotechnol. 21, 885–890.

Yamashita, K., Tachibana, Y., Ohkura, T., and Kobata, K. (1985). Enzymatic basis for the structural changes of asparagine-linked sugar chains of membrane glycoproteins of baby hamster kidney cells induced by polyoma transformation. J. Biol. Chem. 260, 3693–3969.

Zurita, A.J., Arap, W., and Pasqualini, R. (2003). Mapping tumor vascular diversity by screening phage display libraries. J. Control. Release 91, 183–186.

Address reprint requests to:
Dr. Shun'ichi Kuroda
Department of Structural Molecular Biology
Institute of Scientific and Industrial Research
Osaka University
8-1 Mihogaoka
Ibaraki, Osaka 567-0047, Japan

E-mail: skuroda@sanken.osaka-u.ac.jp

Received for publication March 25, 2008; accepted after revision June 25, 2008.

Published online: August 15, 2008.